Topology- and Feature-based Flow Visualization: Methods and Applications

C. Garth[*] *and X. Tricoche* [†]

1 Introduction

The ongoing strive for improved efficiency, performance, and safety is at the core of technical flow design. Typical examples of such flows can be found at all scales, ranging from the gas-burning chamber in household heating appliances that depends on an optimal mixture of oxygen and gas, to high-performance aircraft design. In the recent past, computers have become powerful enough to be truly instrumental in this field, primarily through the widespread use of Computational Fluid Dynamics (CFD). This methodology offers new means to rapidly simulate and evaluate new designs. Moreover, it allows for unprecedented insight into complex fluid dynamics phenomena observed in practical experiments by generating very high resolution data sets that accurately reproduce the entirety of the flow. This evolution emphasizes the need for analysis tools that are both effective and efficient. Scientific Visualization has become essential in this context.

The dedicated research effort is called Flow Visualization. Its major task is to provide tools that allow the user to visually explore and assess the properties of the ever-increasing amount of numerical information that results from CFD computations. One classical approach is to focus the visualization on features of interest that engineers and fluid dynamicists consider essential for both scientific and industrial applications. Prominent examples are vortices, shock waves, and separation or attachment lines. The corresponding visualization techniques are very useful in practice because they yield a simplified representation of involved flow phenomena made of patterns that directly match the intuition of the observer. Their limitation, however, follows from the loose notion of feature that, in most cases, is essentially application specific. In general, different methods rely on different (if not contra-

[*]AG Computer Graphics & Visualization Group, Univ. of Kaiserslautern, Germany (garthinformatik.uni-kl.de)

[†]Scientific Computing and Imaging Institute, Univ. of Utah (tricochesci.utah.edu

dictory) definitions of the same feature and therefore yield heterogeneous results. Vortices constitute a typical illustration of that problem: many definitions have been proposed over the years but none of them is able to properly characterize vortices in all types of flows [8]. Following a different approach topology-based methods extract global flow structures defined with respect to the limit sets of streamlines. The corresponding techniques are built upon the rigorous mathematical formalism of the qualitative theory of dynamical systems, which guarantees objective results. Unfortunately, the connection between topological structures and the practical properties of the flow is sometimes unclear and the resulting pictures tend to lack the intuitive appeal of feature-based representations.

The objective of the paper is two-fold. First, it provides an introduction to state-of-the-art feature and topology-based flow visualization methods. Beyond the techniques traditionally used in practice it describes recent contributions made by the authors, following an approach aimed at combining the strengths of both topological and feature-based techniques to yield more effective visualizations. Second, it demonstrates the use of these algorithms for practical applications. In particular it discusses their ability to meet the needs raised by the analysis of large-scale multi-field CFD data sets.

The contents of this paper are organized as follows. Our description starts with on overview of feature-based flow visualization techniques in section 2. We focus our presentation on the feature types that are most prominent in practice. Topology-based methods are introduced in section 3. Basic notions are defined along with algorithms relevant for visualization purposes. After these initial considerations we adopt a more practical viewpoint and consider successively two different visualization applications. One concerns vortex breakdown analysis, as discussed in section 4. The other is dedicated to flow analysis and optimization in engine components, section 5.

2 Feature-based Visualization

The goal of feature-based visualization methods is to generate images that restrict the depiction of complex flow data to a limited set of points, lines, and volumes representing features of particular interest for the considered application. This yields fairly abstract pictures that convey significant flow properties in a concise and compact form. The most prominent examples of features in CFD applications include vortices, separation and attachment lines, shock waves and recirculation zones.

The loose, empiric nature of the definition of those feature explains the variety of algorithms available to locate, identify, and visualize them and requires the user to determine experimentally which method is best suited for the needs of his particular application. Further restrictions on the type of method can be imposed by the size or the structure of the data.

In this section we present visualization methods dedicated to vortices on one hand,

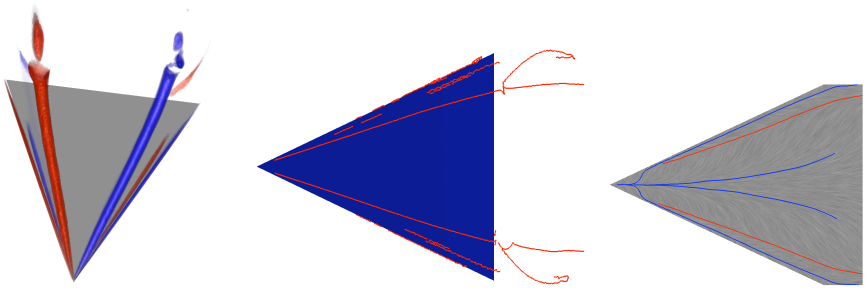

Figure 1. *Samples of feature-based visualization methods.* ***Left:*** *Volume rendering of the λ_2-criterion to illustrate vortices above a delta wing.* ***Middle:*** *Vortices as extracted by the Sujudi-Haimes algorithm. Note the false positives and the generally bad quality of the results.* ***Right:*** *Separation and attachment lines of the shear flow on the wing surface, computed using the scheme from[19] (cf. 4 for a detailed discussion of this dataset).*

and separation and attachment lines on the other hand. This choice is motivated by the major practical significance in practice as explained below and illustrated in sections 4 and 5. For a more general introduction to the topic of feature-based visualization, refer to [11].

2.1 Vortices

The extraction of vortical structures has been a major topic in visualization for quite some time. Although a vortex is most intuitively conceived as the superposition of a flow along an axis and a flow around this axis, there is no satisfying and objective definition that exists for this flow pattern. As a result, vortex extraction methods are essentially characterized by the type of vortex criteria they are built on. This is either a region-based criterion (identifying regions of vortical flow behavior) or a line-type description (focusing on the vortical axis or vortex core line). Region definitions include high vorticity, helicity, low pressure. Most often used in engineering is the λ_2 definition by Jeong and Hussain [5]. The physical meaning behind this method is a similarity measure of the local flow structure to that induced by a pressure valley line. The major limitation of λ_2, however, lies in its incapacity to isolate individual structures.

Among the line-type definitions, the approach of Sujudi and Haimes [14] is most widely used. The idea here is to perform on a cell-wise basis the pattern matching of a rotation motion on the vector field and to extract locally sections of the rotation axis that can be patched together to approximate the vortex core line. Because of the linear nature of the sought pattern, the method has issues with vortex core lines that are strongly curved. Roth and Peikert proposed a higher-order scheme that can extract curved core lines reliably [12]. They also showed in a subsequent paper that this and other similar methods can be formulated in a unified framework involving their *parallel operator* [10].

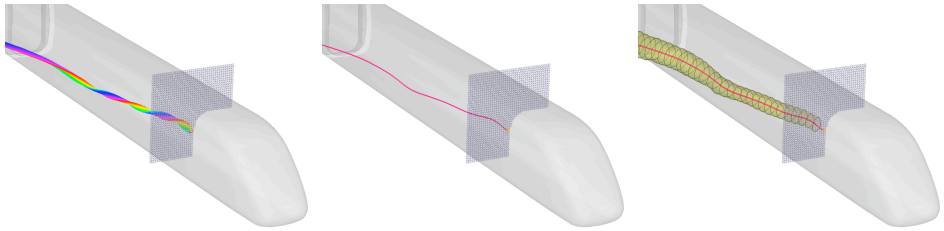

Figure 2. *An illustration of the vortex extraction algorithm from [3].* ***Left:*** *Manually seeded stream surface showing vortical behavior.* ***Middle:*** *Stream surface medial axis as a smooth approximation to the vortex core line.* ***Right:*** *Vortex surface grown outward from the medial axis.*

Additionally, some approaches try to identify a vortical or swirling flow behavior by examining the evolution of particles [6]. Recently, Garth et al. presented a more general stream surface[1]-based approach [3] that allows for the extraction of a vortex core line approximated as the medial axis of a stream surface that exhibits vortical behavior. The stream surface can be seeded along a closed curve surrounding the center of a two-dimensional rotation identified on a probing plane that the user can position arbitrarily in the flow. The starting curve can also be adjusted to the vortex core line approximation provided by another scheme. The authors combine this technique with a region-growing algorithm that relies on a common vortex model from fluid dynamics to identify a vortex region. Overall this method proves significantly more robust than alternative solution when applied to slowly swirling vortices. An overview of the successive steps of the method is proposed in Fig. 2.1.

While most of the methods mentioned above provide satisfactory visualizations for simple datasets, the extraction of vortices in modern CFD datasets remains essentially challenging and a significant amount of user interaction is required to obtain useful results.

2.2 Separation and Attachment Lines

Separation and attachment lines are another major feature type. They are defined as the lines along which the flow attaches or separates from the surface of an embedded body (e.g. an aircraft). This phenomenon is induced by viscous effects that take place in direct proximity of the object. In that setting, the flow has so-called no-slip boundary condition which means that the velocity magnitude goes to zero as one approaches the surface along a normal direction. Therefore, the analysis is focused on the non-zero, tangential shear-stress vector field defined over the surface that exhibits the same flow patterns as nearby located streamlines. In particular flow separation and attachment induce the creation of curves of asymptotic streamline

[1] A stream surface is the surface spanned by an infinite set of streamlines starting on an arbitrary seeding curve

convergence which are visible in the shear stress vector field. The corresponding three-dimensional flow pattern is characterized by the presence of a stream surface starting or ending along the feature line that, on the other hand, swirls around a nearby located vortex. As a matter of fact, flow separation and vortex genesis are two closely related phenomena.

Following the original idea of Sujudi and Haimes for vortex core lines, Kenwright et al. proposed a simple and fast method for the extraction of separation and attachment lines [7]. Their basic observation is that these feature lines are present in two linear patterns, namely saddle points and nodes (see section 3), where they are aligned with an eigenvector of the Jacobian. The original method works on a cell-wise basis and extract these pattern within each triangle. Hence it results in disconnected line segments, caused to the discontinuity of the Jacobian. Yet, applying the parallel operator leads to the reformulation of the features in terms of lines of zero curvature and yields connected lines. However this definition is quite restrictive because it assumes that separation resp. attachment lines always have zero curvature. Moreover, since it requires derivative computation it is very sensitive to noise. Consequently strong pre-smoothing of the data is often necessary which in turn can deform and shift the features. Another approach was proposed earlier by Okada and Kao [9] who extend the classical Line Integral Convolution (LIC) algorithm [1] by color coding the flow direction so as to highlight the fast changes in flow direction that occur as streamlines approach separation resp. attachment lines. The weakness of this approach lies in the heavy computation associated with LIC on one hand, and in the fact that the geometry of the feature lines is not extracted. Instead, the method computes a density function that indicates the proximity / likelihood of these feature lines.

Using a different approach, Tricoche et al. recently proposed a scheme [19] designed to overcome the restrictions imposed by the purely local analysis used in the algorithms mentioned previously. Their method can be decomposed in three stages. The first one applies a local criterion to estimate the likelihood of each grid vertex to lie close to a separation resp. attachment line. In essence, this stage is comparable to the method of Okada and Kao [9]. However the density computed here is not directly visualized but serves as input for the next step of the algorithm. Moreover the local criterion used can be chosen arbitrarily by the user. In particular, the pattern matching idea underlying Kenwright's method [7] can be reformulated to yield a distance value. The second step leverages these local estimates to monitor the global convergence of streamlines toward separation resp. attachment lines. This step is justified by the asymptotic streamline convergence that takes place along separation and attachment lines in the shear stress vector field. Observe that streamline integration is global in nature, which makes the method both more robust and more flexible than Kenwright's approach. Practically, the ridge and valley lines of the density function computed previously are extracted. The resulting skeleton is then used to restrict the candidate seed points for streamline integration to a set of isolated lines that are discretized at a predefined resolution. Streamline convergence is measured on a cell-wise basis by incrementing a local counter every time a streamline crosses a cell. The final step consists in extracting the ridge and valley lines of this convergence map. This yields an approximation of the location

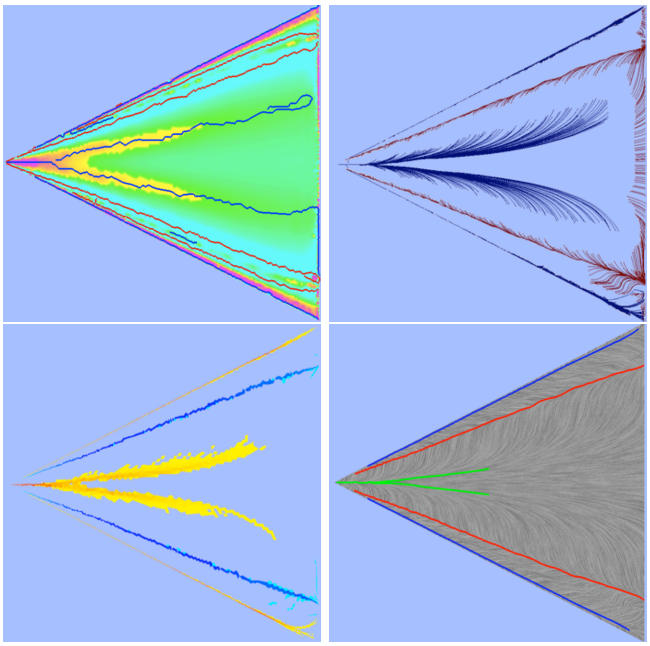

Figure 3. *Successive steps of the extraction method for separation and attachment lines [19].* ***Top left:*** *ridge and valley lines of density function.* ***Top right:*** *streamlines seeded along ridge and valley lines.* ***Bottom left:*** *cell-wise accumulation monitoring.* ***Bottom right:*** *separation and attachment lines.*

of separation and attachment lines, the accuracy of which is determined by the grid resolution. The actual geometry is eventually provided by streamline integration. An overview of these successive steps is shown in Fig. 3.

3 Topology-based Visualization

Vector field topology is a powerful approach for the visualization of planar flows. Topology-based methods leverage basic results of the qualitative theory of dynamical systems to generate effective depictions characterized by a high level of abstraction and an accurate segmentation of the domain in regions where the flow exhibit a uniform behavior. Formally, this classification is defined with respect to the limit sets of the streamlines. Additionally, parametric topology and the notion of bifurcation can be used to extend this technique to time-dependent flows and account for the structural transformations that their topology undergoes over time.

Unfortunately, the application of this methodology to three-dimensional problems has not so far demonstrated the same usefulness in visualization applications. One explanation is the intricacy of the resulting pictures: the topology of volume flows involve stream surfaces that are plagued by self-occlusion and visual clutter.

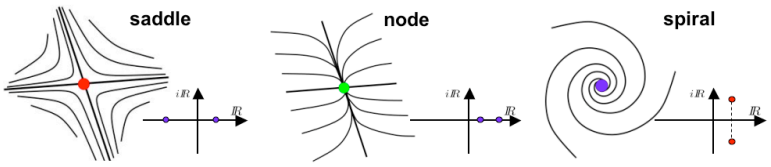

Figure 4. *Linear planar critical points*

Another problem concerns the lack of intuitive connection between topological structures and major features of interest in fluid dynamics problems, as described in the previous section. Neither vortices nor separation lines are, in general, topological in nature. Thus topology-based methods fail to extract them properly.

In the following we provide a short introduction to essential notions of planar and three-dimensional vector field topology. Our presentation is driven by the needs of visualization algorithms discussed in the next section. For a more complete survey of existing methods in topology-based flow visualization, we refer the reader to [13].

3.1 Topological Skeleton of Steady Flows

The topology of a vector field is the decomposition of its phase portrait into regions where all streamlines have the same limit sets. The *phase portrait* considers all points located along the same streamline as a single equivalence class. In other words, it interprets the domain in terms of its dense coverage by streamlines. A *limit set* is defined as a set of points that constitute the asymptotic limit of a streamline, either forward or backward. We restrict our considerations to the two most common types of limit sets: critical points and cycles.

Limit Sets

The *critical points* of a steady vector field are the locations where the field magnitude vanishes. Because of the uniqueness of the solution of a dynamical system with respect to its initial conditions, critical points are the only locations where streamlines can meet asymptotically. In the non-degenerate, linear case, the nature of a critical point is determined by the eigenvalues of the Jacobian matrix. The different types are illustrated in Fig. 4 and Fig. 5 for the planar and three-dimensional case, respectively. In both cases, the eigenvalues are shown along with the associated configuration. When all the eigenvalues have positive (resp. negative) real parts, the critical point is a source (resp. sink). If both positive and negative real parts are present, the critical point exhibits both source and sink behavior and is called a saddle point.

Cycles are closed streamlines that correspond to periodic solutions of the dynamical system. The non-degenerate case corresponds to cycles that act as sink or sources with respect to the surrounding streamlines.

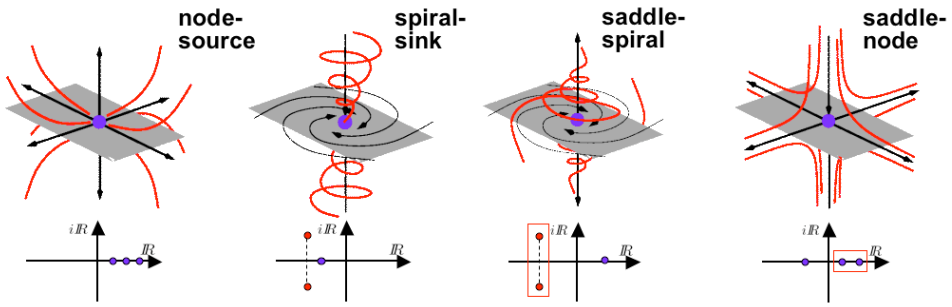

Figure 5. *Linear critical points in three-dimensions*

Separatrices

The limit sets present in a vector field induce a segmentation of the domain into regions where all streamlines share the same limit sets for forward and backward integration. The boundaries between such regions are called separatrices.

Specifically, in the planar case two major types of separatrices exist: cycles and streamlines that attach to a saddle point along its eigenvectors. Refer to Figure 4. As in the planar setting, separatrices of the three-dimensional topology are either periodic manifolds or they start at saddle points along their eigenvectors. However these separatrices are either 1D (streamlines) or 2D (stream surfaces). The latter are spanned by both eigenvectors associated with the eigenvalues whose real parts have same sign. Again, refer to Fig. 5.

3.2 Topology Extraction

In practice critical points are extracted on a cell-wise basis. In the piecewise linear case, the equation to solve in each cell to determine the position of a zero vector is linear. In the planar, bilinear case, the same problem leads to a quadratic equation. Trilinear interpolation requires numerical schemes like Newton-Raphson to locate critical points. If such a point is found in the interior of a given cell, its type is determined by solving the associated Eigensystem. In the case of saddle points, this analysis also provides the eigenvectors along which the integration of separating streamlines or stream surfaces is carried out.

The extraction of cycles is more involved. Wischgoll and Scheuermann proposed the first method for that purpose [20]. The basic idea of their algorithm is to first identify a cell-wise cycle in which a streamlines appears to be captured. The next step consists in verifying this property by integrating streamlines from the boundary of the cell cycle to ensure that the vector field does indeed prevent any streamline from leaving the corresponding region. This result is then combined with the Poincare-Bendixson theorem which states that in the absence of any critical point in the cell cycle, the limit set present in this region must be a cycle. A method derived from the same principle was later proposed by the same authors for the 3D case [21]. Observe that tori that are stable under the flow are another

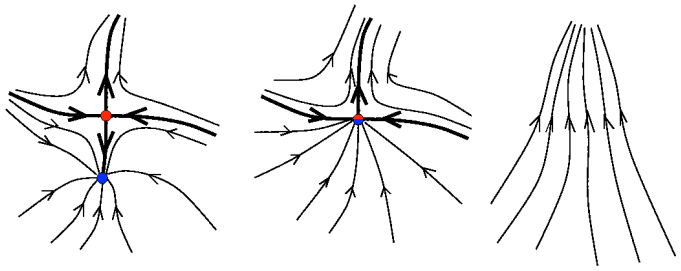

Figure 6. *Fold bifurcation*

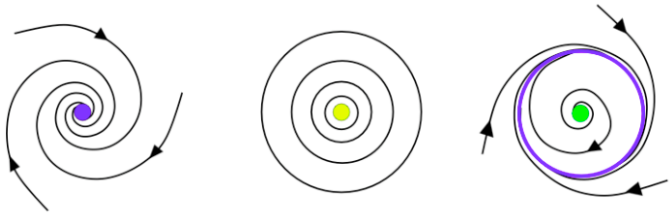

Figure 7. *Hopf bifurcation*

possible generalization of cycles in a three-dimensional setting.

3.3 Parametric Topology and Bifurcations

When a vector field depends on a parameter (e.g. time), changes in the parameter value induce changes to its topology. These transformations are called bifurcations and exist in an infinite variety. Their common property nonetheless is to replace a stable structural configuration by another stable configuration through an instantaneous, unstable pattern. Here, stability is defined with respect to the ability of a given structure to remain qualitatively unchanged after a small but arbitrary modification of the vector field. Bifurcations are either local or global depending on the extent of the region they impact.

For the need of this presentation, we consider only local bifurcations. The most common ones in the planar case fall in two categories: fold and Hopf bifurcation. The former corresponds to the pairwise annihilation (resp. creation) of a saddle point and a sink or source. An example is shown in Fig. 6. The latter is characterized by the transformation of a sink into a source (and vice versa) and the simultaneous creation (resp. annihilation) of a cycle surrounding the critical point. See Fig. 7.

Similar transformations occur in the 3D case. A simple example can be derived from a 2D fold bifurcation by adding a one-dimensional source behavior to a saddle point and a source affected by the transformation. This creates two 3D saddle points that merge and vanish in the very same way. This is illustrated in Fig. 8.

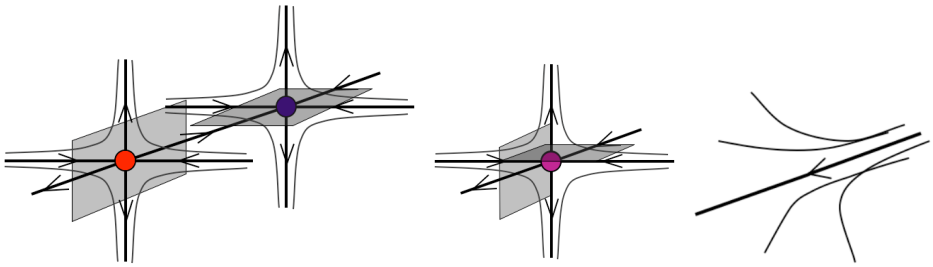

Figure 8. *Three-dimensional fold bifurcation*

3.4 Topology Tracking

A simple algorithmic solution to track the continuous evolution of the topology and detect the associated bifurcations was proposed by Tricoche et al. in [16]. The method was designed for two-dimensional unsteady flows. Its basic idea is to embeds the discrete space-time domain of the data in a three-dimensional grid. More precisely, assuming that the grid is a fixed triangulation, each triangle is expanded along the time axis which creates a prism that connects two consecutive time steps. In each prism, a linear interpolant along the time axis extends to 3D the planar, piecewise linear interpolation defined at each time step.

In this prism grid, the singularities are tracked in a cell-wise manner. Given a critical point present in a cell at a time step the algorithm uses the equation of the 3D interpolating function to determine the path of this critical point throughout the prism. Observe that the interpolation is chosen such as to ensure that at most one critical point is present in a cell at any given time. Therefore only two cases are possible for this path: it can either cross the prism from one time step to the next (i.e. move within the same triangle cell in a 2D perspective) or cross the side faces of the prism before reaching the next time step (that is, leave the triangle where it was located initially between two time steps). When a critical point leaves a prism, its path must be followed further in the corresponding neighbor.

As far as bifurcations are concerned, they can take two forms in that framework. The only local bifurcation that can occur in the interior of a cell (thus involving a single critical point) is a Hopf bifurcation. It is detected by checking the persistence of the sink/source type of the critical point along its path. The cycle originating at the bifurcation point can be tracked by extracting it at each subsequent time step using the scheme of Wischgoll and Scheuermann [20]. Fold bifurcations are constrained to take place on the side faces of a prism. In that case, the path of a saddle point contained in a prism connects with the path of a sink (resp. source) located in a neighboring prism. As explained previously, this configuration can either cause the creation or the annihilation of both critical points. The separatrices emanating from a saddle point can be integrated at each point along the path and reconnected along the time axis to span surfaces in the space-time domain.

The extension of this scheme to three-dimensional vector fields was described by Garth et al. in [4]. The basic idea is the same as in the 2D case. However the space-time domain is decomposed into 4D simplices in their implementation. This choice greatly simplifies the equations to be solved to track the critical points and determine their type everywhere along the time axis. The application of this method to the temporal analysis of a vortex breakdown bubble is discussed in section 4.3. Remark that an alternative technique for topology tracking in two and three dimensions called *Feature Flow Field* was proposed by Theisel and Seidel [15]. However, their method requires all time steps to be available in memory at once which makes it non suitable to handle the large data sets considered in the next section.

3.5 Cutting Plane Topology

To finish this overview of topology-based flow visualization methods, we briefly present a technique called *Cutting Plane Topology* introduced recently by Tricoche et al. [18]. It is based on the topology tracking algorithm mentioned previously and permits to extract and explore complex three-dimensional flow structures. Specifically, a steady three-dimensional flow is investigated through the parametric topology of its 2D projection onto a plane that is swept along a prescribed curve across a volume of interest. In other words, the curve controls how the cutting plane is moved to span a 3D volume and is interpreted as the parameter space for topology tracking. The choice of this curve is therefore application specific. We describe in section 4.2 how the inherent symmetry of the considered flow structures can be exploited to create effective visualizations that unravel intricate flow structures. Another important aspect to consider here is the orientation of the plane as a continuous function of its position along the curve. Once again this choice must be dictated by the flow to yield meaningful results. The solutions proposed in [18] range from a fixed orientation imposed by a symmetry axis to a direction chosen in order to maximize the amount of flow crossing the plane. Once the curve and the plane orientation have been decided, topology tracking can be carried out in a computational space where the successive positions of the plane and the associated sampled vector values are aligned to satisfy the original configuration of [16]. The extracted paths and bifurcations often require low-pass filtering in post-processing to discard the short-term artifacts introduced by the choice of plane orientation. Additional details can be found in [18].

4 Vortex Breakdown Analysis

4.1 Background

In both the civil and military fields, the demand for shorter flight times and faster aircrafts has been a driving force behind research in recent years. Although it is not a recent development, together with supersonic speeds becoming more attractive, the delta wing design has found its way back into aircraft construction, as is demonstrated by a number of military aircrafts and the transatlantic passenger jet Concorde. An increased perception of security and the ever-shortening take-off

and landing intervals on modern airports mandate a thorough examination of delta wing configurations with the aim of controllable flight even in exceptional flight situations, e.g. at a high angle of attack at subsonic speed. Furthermore, in military airflight, exceptional maneuverability is of prime importance. Due to this, the understanding of flow phenomena related to delta wing setups has become a major point of research activity. Among the most interesting of these is *v*ortex breakdown due to its severe impact on flight stability. Delta wing designs differ from more conventional wing designs in that a substantial part of the lift on the wing is not only created by Bernoulli's principle (i.e. the velocity and hence pressure difference above and below the wing), but by large vortex systems above the wing. Breakdown of these vortices, i.e. the sudden loss of coherent vortical flow structures above the wing, can have catastrophic consequences, due to the sudden loss in lift and structural failure of the wing construction. While the phenomenon has been known for quite some time, there is still a lack of good theories of its genesis. Numerical research can be extremely helpful in allowing to study the occurrence of vortex breakdown in computer simulations. In the following, we describe a dataset from a simulation of a delta wing configuration that exhibits breakdown and apply a number of visualization techniques to study it.

The dataset results from an unsteady computation of the Navier-Stokes equations in a volume surrounding a delta wing. As the simulation progresses, the angle of attack increases. The data is given on an unstructured adaptive-resolution grid with about 12 million cells and includes 1000 time steps. This dataset poses a significant challenge for visualization algorithms, owing to both size and numerical resolution issues.

4.2 Formation of Vortex Systems

In order to verify the correctness of the simulation and get an insight into the vortex systems above the wing, the extraction of vortices above the wing surface is an important task. The vortices above the wing actually form two symmetric vortex systems consisting of primary, secondary and tertiary vortices each.

Figure 9 (left) provides an overview showing the basic configuration. A stream surface started just below the wing apex illustrates the flow of air going over the edges and rolling up into the two primary vortices. The right image provides a view of the same surface from an opposing angle, revealing the three vortices on each side of the wing. It is interesting to note that while the primary and secondary vortices are almost circular in shape, the tertiary vortex is extremely elliptic. In the left image,another pair of stream surfaces wraps around the primary vortex core lines and exhibits spiraling behavior, as illustrated by proper color coding. About two thirds along, the coherent motion of these surfaces is interrupted and replaced by a bubble shaped structure. Despite the general symmetry of the dataset, the vortex breakdown it exhibits is asymmetric. On the (in direction of flight) right side, a so-called *breakdown bubble* forms, while the left-side structure looks chaotic.

The stream surfaces make for a good illustration of the major phenomena in the dataset. Since the vortex axes move over time, the seeding curves for the streamlines need to be determined manually for every time step, which is tedious.

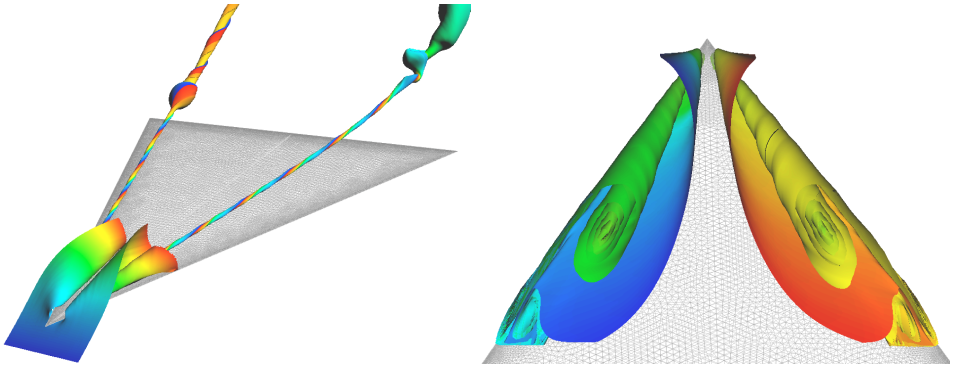

Figure 9. ***Left:*** *Overview of the delta wing dataset with vortex creation at apex and the two primary vortices, breaking down differently.* ***Right:*** *Formation of primary, secondary and tertiary vortices at wing apex. Note how the shape of the tertiary vortex is strongly elliptic. For both images, the surface color coding depends on the starting curve location of individual streamlines (s-parameter).*

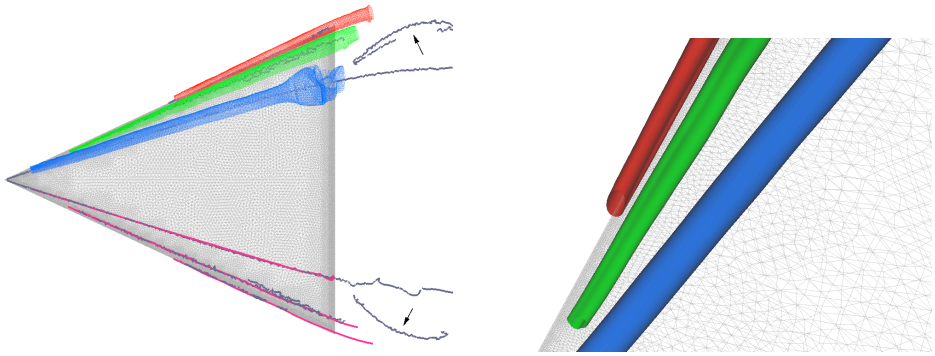

Figure 10. *Vortices as extracted by the vortex surface technique. False positives (indicated by arrows) are reliably discarded. The closeup (right image) shows clean separation between the three vortices that form the vortex system. Note the strongly elliptic shape of the tertiary vortex (red).*

Automatic vortex core line extraction can help to some extent. Figure 10 (left) shows the results of an application of the Sujudi-Haimes algorithm (dark lines). The results are of mixed quality in that they include the vortex systems as well as some false positives. Using stream surfaces and the vortex surface technique detailed above, it is possible to discard the false positives, extract smooth vortex core lines (magenta lines) and obtain good vortex regions for each of the three vortices (red, green and blue surfaces). The right image shows a closeup. The separation between the individual vortices is excellent, and the elliptic shape of the tertiary vortex is extracted well.

To further understand the relation between the different vortices in each sys-

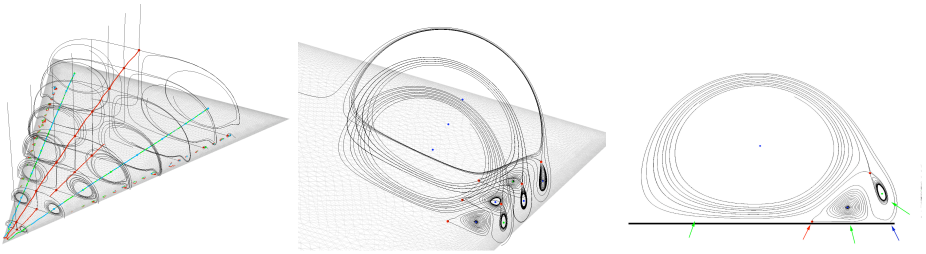

Figure 11. *Application of cutting-plane topology to a delta wing simulation.* ***Left:*** *Plane travels along the wing symmetry axis, revealing the primary vortices and extracting their core lines as spiral-type critical point paths.* ***Middle:*** *Plane travels along the primary vortex core line. The full vortex system is visible.* ***Right:*** *A single slice (from the middle image) allows a detailed observation of the structural interaction between different vortices (marked by green arrows) and the corresponding separation and attachment (see also Fig. 12) on the wing surface (blue and red arrows).*

tem, we have applied cutting-plane topology. The resulting structures are shown in Figure 11. The left image gives an overview of the structures that are revealed when the cutting plane travels along the symmetry axis of the wing. Although it is not orthogonal to the vortical structures, a good overall picture of the flow situation results. The primary vortex cores can be identified as the paths of critical points as the plane travels. The middle and right images show a closeup of the vortex system structure. More detail is extracted as the plane travels orthogonal to the primary vortex core. The interaction of the different vortices can be inferred from the topology. Effectively, the visualization of the vortex system is here reduced to two-dimensions, where it is much easier to comprehend. The separation in the wing shear flow appears as a natural part of the vortex system (individual vortices indicated by green arrows) and is extracted as the paths of saddle critical points close to the wing surface (red arrow in the right image). This *primary separation* is essentially the boundary of the influence regions of the primary and secondary vortices.

The separation and attachment structures can also be extracted directly, although with some difficulty. Figure 12 (left) shows results obtained using the approach described in Section 2. The primary separation is clearly visible. Together with the topological visualizations presented before, a complete picture of the complex vortex dynamics above the delta wing can be obtained and compared to a theoretical model (cf. [2]). Although it is not of direct use in the analysis of vortex breakdown, it is of great value with respect to a validation of simulation results. In the next section, we focus on a direct visualization of the breakdown structure.

4.3 Structure and Evolution of the Breakdown Bubble

The complicated structure of the breakdown bubble presents a serious challenge for established visualization techniques. Since it is three-dimensional in nature, naive geometric visualizations such as using streamlines suffer from issues of spatial

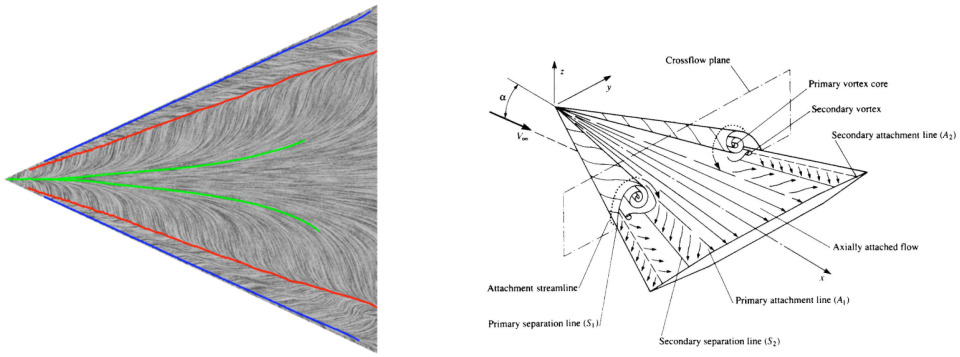

Figure 12. ***Left:*** *Separation and attachment lines in the wing shear flow as extracted with the method from [17].* ***Right:*** *Illustrative sketch of the three-dimensional flow structure above a delta wing and the resulting shear flow structure on the wing (from [2]).*

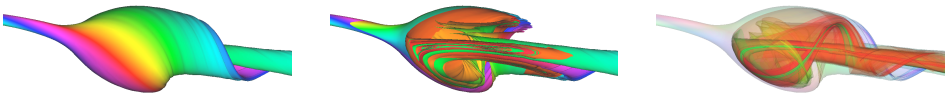

Figure 13. *A stream surface illustrating the flow structure of the breakdown bubble in the delta wing dataset. While the opaque rendering (left) fails to provide insight, application of a clipping plane (middle) or transparent rendering (right) details the internal flow structure, essentially consisting of an asymmetric recirculation zone rotating around the original vortex core line.*

perception issues. Stream surfaces can deliver better images here by providing a surface primitive that helps in understanding the three-dimensional structure of the flow. Fig. 13 provides an example. While the stream surface completely wraps the breakdown bubble, inner structure is easily revealed by applying a clipping plane. The observed motion is of a recirculation-type, overlaid by a simultaneous rotation around the original vortex axis.

To better identify the recirculation zone, cutting-plane topology is an ideal tool as it allows to discard the superposed rotation. In this case, the cutting-plane rotates on the vortex axis. The recirculation can easily be identified by a closed, strongly curved vortex core (cf. Fig. 4.3) that appears as a spiral-type critical point path in the cutting-plane topology. It is interesting to note that these recirculation vortices are very hard to extract using conventional schemes due to their strongly curved nature. The right image shows three recirculation zones, hinting at several occurrences of vortex breakdown of the primary vortex. While the cutting-plane topology is immensely useful in the analysis of the breakdown bubble flow structure, it cannot provide an understanding of the dy-

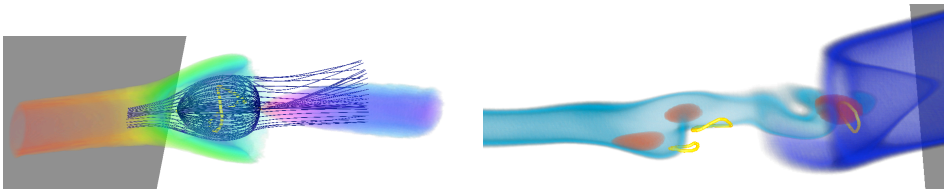

Figure 14. *Application of cutting-plane topology to vortex breakdown analysis. Visualization of topology is enhanced by volume-rendered isosurfaces of velocity magnitude.* ***Left:*** *Right-side breakdown bubble. Structure is revealed through cutting-plane topology (plane revolving on vortex axis). The recirculation core is extracted as a spiral-type path (yellow).* ***Right:*** *Left-side staggered breakdown. Although a breakdown bubble is not discernible, several recirculation zones are extracted (yellow), hinting at multiple breakdown bubbles.*

namic of the flow in this case since it is essentially limited to a single time slice. Topological methods can still be useful in this context. It has been known that the occurrence of a breakdown bubble is accompanied by stagnation points in the flow, i.e. critical points of the flow vector field, that lie on the vortex axis and essentially "delimit" the bubble. While these critical points are of saddle-type, topological visualization of the separating surfaces is essentially equivalent to a direct application of stream surfaces (Fig. 13). It is interesting, however, to apply critical-point tracking in this context. Although the resulting visualization is essentially four-dimensional (the critical points move in three-dimensional space over time), it can be reduced to two dimensions by observing that the movement of the stagnation points is limited to the axis of the primary vortex. The benefit of this procedure is twofold: First, the resulting structural graph allows to infer the structural evolution over all time steps. Second, since the dataset under consideration is asymmetric, it provides a simple and effective means to compare the evolution on both sides (Fig. 15). Comparing these results with those from Fig. 4.3 confirms that the left-side breakdown is chaotic (several small rapidly oscillating bubbles).

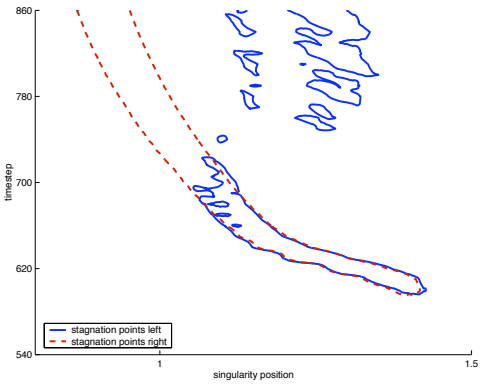

Figure 15. *Structural graphs of left (blue) and right (red) side breakdown bubble evolution. While both sides start out almost identically, the left side deteriorates into chaotic breakdown and shows several rapidly oscillating bubbles in later time steps.*

5 Evaluation of Flow in Engine Components

With the general progress of state-of-the-art CFD simulations, the discipline of engine design is made accessible to both numerical simulation and visualization of the resulting datasets, allowing for rapid testing of engine designs. In the following we give an example of the application of topological and feature-based visualization methods for the analysis of prototype simulations.

Among the many design goals of combustion engines, the mixing process of fuel and oxygen occupies an important place. If a good mixture can be achieved, the resulting combustion is both clean and efficient, with all the fuel burned and minimal exhaust remaining. In turn, the mixing process strongly depends on the inflow of the fuel and air components into the combustion chamber or cylinder. If the inlet flow generates sufficient kinetic energy during this valve cycle, the resulting turbulence distributes fuel and air optimally in the combustion chamber. For common types of engines, near-optimal flow patterns are actually known and include, among others, so-called swirl and tumble motions. We show two examples of simulation datasets showing each of these two types of flow patterns (henceforth termed "swirl-motion" and "tumble motion"). The basic geometries of the datasets and the respective desired motion patterns are shown in Figure 16.

Diesel Engine
This simulation is the result of a the simulation of steady charge flow in a diesel engine, based on a stationary geometry, resulting in a simple and stable flow. The main axis of motion is aligned with the cylinder axis and is constant in time. The spatial resolution of the single time step is high with a total of 776,000 unstructured cells on an adaptive resolution grid.

Gas Engine
This dataset results from an unsteady simulation of the charge phase of a gas engine. As the piston moves down, the cylinder volume increases by an order of magnitude and the fuel-air mixture entering the cylinder is drawn into a gradually developing tumble pattern. The overall motion is highly transient and unstable. Both spatial and temporal resolution are relatively low, with the data given on 32 time steps and the grid consisting of roughly 61,000 unstructured elements at the maximum crank angle.

For both datasets, the simulation results are given in the form of a vector field defined in the interior of the respective cylinder geometries. As is quite common in CFD simulations, the flow is required to vanish on the domain boundary (the so-called *no-slip boundary condition*) in order to correctly model fluid-boundary friction. Nevertheless, values on the boundary of the domain are easily inferred by e.g. extrapolation of volume values next to the boundary. We remark that in classical automotive engineering analysis, visualization is rarely performed for volume or boundary data but instead on two-dimensional slices. The main visualization goal in these cases is is the extraction and visual analysis of the swirl- and tumble-motion patterns.

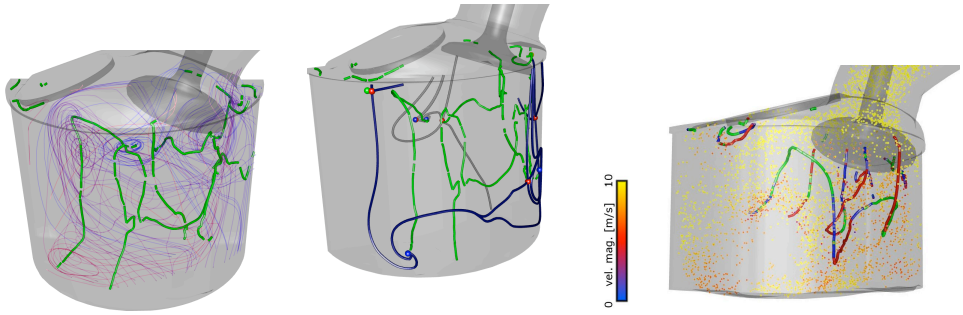

Figure 17. *Application of cutting-plane topology and boundary topology to the gas engine dataset.* ***Left:*** *Cutting-plane topology provides a good overview of the overall motion pattern. Spiral-critical point paths (green) indicate rotation centers.* ***Middle:*** *In combination with boundary topology, interactions of boundary and volume flows are visible. Spiral critical points occur on the boundary where vortices intersect it.* ***Right:*** *Rotational centers enable an enhanced interpretation of conventional particle visualizations. Particles are color coded according to velocity magnitude. It is visible how the rotation centers capture particles in small-scale rotations.*

Unlike the previous dataset, in these datasets methods for the extraction of separation and attachment lines could not be applied since the resolution of the boundary flow field is too low. However, in our experiments we found that boundary topology is successful in extracting separation and attachment structures in the boundary fields due to the existence of critical points. In combination of with cutting plane topology, it is an effective approach to the extraction of swirl or tumble patterns and gives a good impression of the mutual influences of boundary and volume flows. Figure 17 illustrates this in a single time-slices of the gas engine dataset. From these images, one can recognize that the overall desired tumble motion actually consists of three independent rotational centers that together form the tumble motion. Since one of these vortices is rotating opposite to the other two, the tumble motion is much weaker

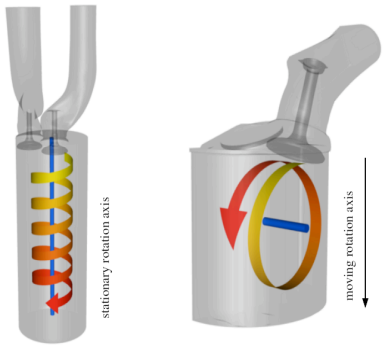

Figure 16. ***Left:*** *Stable, circulating flow pattern in a diesel engine designated as* swirl motion*, with the cylinder axis as the axis of rotation. The flow enters tangentially through the intake ports.* ***Right:*** *Transient tumble motion in a gas engine. The axis of motion moves as the cylinder expands downwards and stays halfway between the top cylinder wall and the piston head at the bottom.*

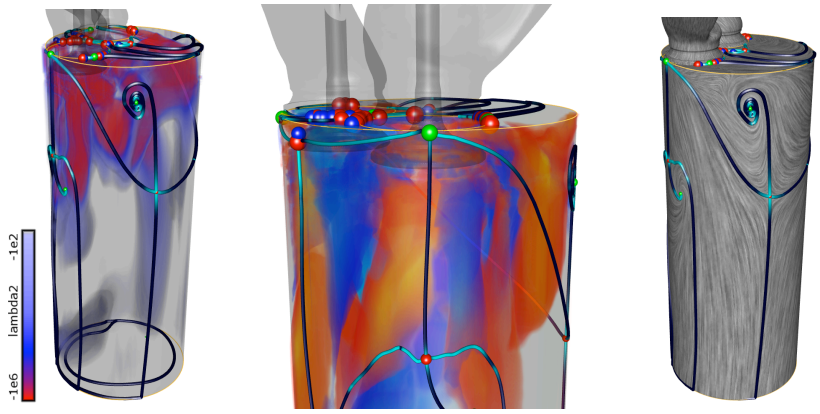

Figure 18. *Visualization results for the diesel engine. Interaction of volume and boundary flows can be observed where separatrices on the boundary indicate a separation between two vortices in the volume close to the boundary.* ***Left:*** *A combination of boundary topology with a volume rendering of λ_2. The transfer function is chosen to indicate rotation strength.* ***Middle:*** *Here, the transfer function is chosen to represent the direction of the rotation (red vs. blue). Counter-rotating vortices close to the cylinder top take away kinetic energy from the formation of the main swirl pattern.* ***Right:*** *Boundary topology laid over a LIC image of the boundary flow.*

than expected, and the design must be improved. Here, the axis for the cutting-plane approach is quite naturally parallel to the desired tumble axis, discarding patterns of motion that are not considered important for this application.

For the diesel engine (where a swirl-type pattern is desired), topological methods can provide results of similar quality, especially in combination with other techniques. Since the topological visualizations are mostly sparse in the sense that they provide a concise line-type depiction of the flow structure, it makes sense to combine them with feature extraction techniques that create a dense visualization (such as the λ_2-criterion) or other visualization techniques. Figure 5 gives several examples of hybrid visualizations of this type. The combination of boundary and volume visualizations gives a good understanding of the general nature of the flow. Again, we find that the overall swirl pattern is a combination of several smaller vortices. There is only one large but weak vortex extending all the way to the bottom of the engine cylinder. The achieved pattern is therefor suboptimal.

For both the gas and diesel engines, the presented visualizations can be constructed without user assistance. This guarantees that visualizations are comparable between different simulation datasets of the same type, an important property when using visualization as a design analysis tool.

Bibliography

[1] B. Cabral and L. C. Leedom. Imaging vector fields using line integral convolution. 1993.

[2] U. Dallmann. Topological Structures of Three-Dimensional Flow Separations. Technical Report 221-82 A 07, Deutsche Forschungs- und Versuchsanstalt fuer Luft- und Raumfahrt, 1983.

[3] C. Garth, X. Tricoche, T. Salzbrunn, and G. Scheuermann. Surface Techniques for Vortex Visualization. In *Proceedings Eurographics - IEEE TCVG Symposium on Visualization*, 2004.

[4] Christoph Garth, Xavier Tricoche, and Gerik Scheuermann. Tracking of Vector Field Singularities in Unstructured 3D Time-Dependent Datasets. In *Proceedings of IEEE Visualization*, pages 329–336, October 2004.

[5] Jinhee Jeong and Fazle Hussain. On the Identification of a Vortex. *Journal of Fluid Mechanics*, pages 69–94, 285 1995.

[6] M. Jiang, R. Machiraju, and D. Thompson. A Novel Approach to Vortex Core Detection. In *Data Visualization 2002*, pages 217 – 226, Aire-la-Ville, Sitzerland, 2002. Eurographics Association.

[7] D. Kenwright, C. Henze, and C. Levit. Feature extraction of separation and attachment lines. *IEEE Transactions on Visualization and Computer Graphics*, 5(2):135–144, 1994.

[8] H. J. Lugt. *Introduction to Vortex Theory*. Vortex Flow Press, Inc., 1996.

[9] A. Okada and D. L. Kao. Enhanced line integral convolution with flow feature detection. In *Proceedings of IS&T/SPIE Electronic Imaging*, pages 206–217, 1997.

[10] R. Peikert and M. Roth. The parallel vectors operator - a vector field visualization primitive. In *IEEE Visualization Proceedings '00*, pages 263 – 270, 1999.

[11] F. H. Post, B. Vrolijk, H. Hauser, R. S. Laramee, and H. Doleisch. Feature Extraction and Visualization of Flow Fields. In *Eurographics 2002 State-of-the-Art Reports*, pages 69–100, 2–6 September 2002.

[12] M. Roth and R. Peikert. Higher-order method for finding vortex core line. In *IEEE Visualization Proceedings '98*, pages 143 – 150, 1998.

[13] G. Scheuermann and X. Tricoche. Topological methods for flow visualization. In C.D. Hansen and C.R. Johnson, editors, *The Visualization Handbook*, pages 341–356. Elsevier, 2005.

[14] D. Sujudi and R. Haimes. Identification of Swirling Flow in 3D Vector Fields. Technical Report AIAA Paper 95–1715, American Institute of Aeronautics and Astronautics, 1995.

[15] H. Theisel and H.-P. Seidel. Feature flow fields. In *VISSYM '03: Proceedings of the symposium on Data visualisation 2003*, pages 141–148, Aire-la-Ville, Switzerland, Switzerland, 2003. Eurographics Association.

[16] X. Tricoche, T. Wischgoll, G. Scheuermann, and H. Hagen. Topology Tracking for the Visualization of Time-Dependent Two-Dimensional Flows. *Computers & Graphics*, 26(2):249 – 257, 2002.

[17] Xavier Tricoche, Christoph Garth, Tom Bobach, Gerik Scheuermann, and Markus Rtten. Accurate and efficient visualization of flow structures in a delta wing simulation. In *Proceedings of 34th AIAA Fluid Dynamics Conference and Exhibit*, June 2004. AIAA Paper 2004 – 2153.

[18] Xavier Tricoche, Christoph Garth, Gordon Kindlmann, Eduard Deines, Gerik Scheuermann, Markus Rtten, and Charles Hansen. Vizualization of Intricate Flow Structures for Vortex Breakdown Analysis. In *Proceedings of IEEE Visualization*, pages 187–194, October 2004.

[19] Xavier Tricoche, Christoph Garth, and Gerik Scheuermann. Fast and robust extraction of separation line features. In *Proceedings of the Dagstuhl Scientific Visualization Seminar*, 2003. to appear.

[20] Thomas Wischgoll and Gerik Scheuermann. Detection and visualization of closed streamlines in planar flows. *IEEE Transactions on Visualization and Computer Graphics*, 7(2):165–172, 2001.

[21] Thomas Wischgoll and Gerik Scheuermann. Locating closed streamlines in 3d vector fields. In *VISSYM '02: Proceedings of the symposium on Data Visualisation 2002*, pages 227–ff, Aire-la-Ville, Switzerland, Switzerland, 2002. Eurographics Association.